Protein and lipid enrichment of quinoa (cv.Titicaca) by dry fractionation. Techno-functional, thermal and rheological properties of milling fractions

Ángela García Solaesa, Marina Villanueva, Antonio J. Vela, Felicidad Ronda*

Department of Agriculture and Forestry Engineering, Food Technology, College of Agricultural and Forestry Engineering, University of Valladolid, Spain
**Corresponding author. E-mail: fronda@iaf.uva.es*

Abstract

The quality of quinoa flour is greatly determined by its non-starch components, mainly protein and lipids. Dry fractionation has an important impact on the composition and physicochemical properties of quinoa flour and grits. Quinoa cv. Titicaca, the most extensively grown in Europe and little studied so far, was used in this work. Hydration, techno-functional, rheological and thermal properties of three quinoa fractions obtained by dry fractionation (fine, medium and coarse) were evaluated and related to their particle size and composition. The medium fraction (~500 μm) was enriched in protein (50%) and lipids (80%) and depleted in starch (30%) with respect to the original grain; while the coarse fraction (~1000 μm) was enriched in starch (7%) and reduced in protein (15%). The fine fraction showed the most similar functional, pasting and rheological properties to the whole grain quinoa flour. The coarse fraction led to the most consistent gels, with the elastic (G') and viscous (G") moduli being ten and twenty times higher than those found in the other quinoa fractions and the whole grain flour. The degree of retrogradation as well as the formation of the amylose-lipid complex were markedly affected by the particle size and not so by the composition of each fraction. This work allows to conclude that dry fractionation of quinoa grains is a feasible procedure to tailoring the nutritional profile of the flour and its techno-functional and rheological properties.

***Keywords**: quinoa cv. Titicaca; particle size; milling fractions; functional properties; thermal properties; gels viscoelasticity*

1. Introduction

Pseudocereals are basically starch crops, however they contain important amounts of protein and oil, which often establish their suitability for a particular purpose (García-Salcedo, Torres-Vargas, & Ariza-Calderón, 2017). Quinoa (*Chenopodium quinoa* Willd.) is botanically defined as a pseudocereal native from the Andes. It is considered a whole-grain carbohydrate, as well as a whole vegetable protein being also a gluten-free source. In addition it presents a high quality oil and high levels of vitamins, minerals and a large variety of bioactive compounds (Pereira et al., 2019). Since it has been demonstrated that quinoa shows excellent nutritional properties, around 2000, the interest on it has risen considerably (Jacobsen, 2003). The spread of quinoa around the world is built on its great adaptability to different agricultural growing conditions, hence many countries in different parts of the world have also become producers (Bazile & Baudron, 2013).

The Danish improved cultivar Titicaca (cv. Titicaca) was a hybrid between southern Chilean and Peruvian lines, bred and selected at the University of Copenhagen (Sun, Liu, Bendevis, Shabala, & Jacobsen, 2014). Quinoa cv. Titicaca is the most extensively grown in Europe since it can be cultivated in drought and salt stress conditions of Mediterranean-type agroecosystems (Cocozza et al., 2013). Although quinoa of Andean cultivars is relatively well characterized (Contreras-Jiménez, Torres-Vargas, & Rodríguez-García, 2019; García-Salcedo et al., 2017; Zhu & Li, 2019), so far very little information is available about European quinoa cv. Titicaca (Benito-Román, Rodriguez-Perrino, Sanz, Melgosa, & Beltrán, 2018; Solaesa, Villanueva, Beltrán, & Ronda, 2019).

Quinoa is mostly consumed as a whole grain or milled as a whole flour, after removal of the saponins, either by washing or polishing. These saponins are located in the pericarp, the outer seed layer of quinoa seed (Abugoch James, 2009). Quinoa germ or embryo represents approximately 30% of the whole seed. It surrounds the perisperm like a ring, unlike in cereals, that is found inside the grain representing around 5% of the seed (Mufari, Miranda-Villa, & Calandri, 2018). Starch granules occupy the cells of the perisperm, which constitutes 60% of the grain, while most of the lipids and proteins are located in the germ (Ando et al., 2002; Prego, Maldonado, & Otegui, 1998). This distribution of nutritive compounds within the different tissues is very interesting regarding the obtention of different enriched fractions. Traditionally quinoa is used boiled or toasted, and as whole grain flour in porridge or soups. However nowadays there are increasingly more products made with quinoa, such as pasta, snacks and gluten-free bakery products (Wang & Zhu, 2016) even so special products such as quinoa oil (Benito-Román et al., 2018), edible films or Pickering emulsions, which require a specific formulation (Wang & Zhu, 2016). This wide applicability range derives from its versatility as food ingredient (Pellegrini et al., 2018).

The quality of the products is greatly dependent on the constituents and the particle size of the flour employed. Dough rheology is critical in optimizing product development as it influences the final product quality (Mastromatteo et al., 2012; Sosa et al., 2019). Stikic et al. (Stikic et al., 2012) demonstrated that the addition of quinoa in the form of seeds to wheat flour did not reflect on dough development and stability in contrast to the addition of quinoa flour. The development of gluten-free pasta is an explored application of quinoa to improve its technological and nutritional quality (Sosa, Califano, & Lorenzo, 2019), that requires grits of particle sizes comprised between 200 and 600 μm (Joubert, Morel, & Lullien-Pellerin, 2018).

Benito-Román et al., 2018 and Wejnerowska & Ciaciuch, 2018 found that particle size of quinoa is of paramount importance in the supercritical carbon dioxide extraction of quinoa oil. They studied the effect of particle size distribution of ground seeds in order to increase the extraction efficiency. The best results were obtained for the intermediate particle size (250-500 μm). In those works, the size selection criterion gave priority to mass transfer considerations rather than to the concentration of lipids in the fraction used. The largest particle size (500-1000 μm) presented a higher resistance to the internal mass transfer, and therefore the extraction was very slow; and very small particle sizes, by contrast, induced the channeling of the CO_2, which would leave zones of the packed bed without contact with the solvent. Solaesa et al. (Solaesa et al., 2019) reported the good techno-functional properties of defatted quinoa in the form of grits (500 μm) obtained as a coproduct from quinoa oil supercritical extraction.

In view of the technological interest that quinoa grits of intermedium size (~500 μm) have for different industrial applications, a simple, efficient and fast dry milling process to obtain quinoa grits of this particle size enriched in lipids (supercritical oil extraction) and proteins (pasta

making) has been studied and implemented. The techno-functional, thermal and rheological properties of the enriched milling fraction of ~500 μm and the rest of streams obtained from dry grinding have been characterized. European quinoa cv. Titicaca, little explored so far, has been used in the study. The work will provide an integral knowledge of quinoa applicability based not only on its composition but also on the functionality of the different milling fractions.

2. Materials and methods

2.1 Samples

Seeds of quinoa (*Chenopodium quinoa* Willd.) cv. Titicaca were kindly provided by Extremeña de Arroces (Cáceres, Spain). According to the supplier, saponins were previously removed from quinoa seeds by abrasion polishing (supplier information). Quinoa grains were ground in a ball mill (Pulverisette 6, Fritsch, Germany) following a milling process optimized by Benito-Roman et al. (Benito-Román et al., 2018). The quinoa grits were divided in three fractions: Fine fraction, with a particle size ~200 μm, medium fraction, of ~500 μm, and coarse fraction, of ~1000 μm. The yield of these fractions was 11, 21 and 68% respectively. Likewise, quinoa grains were also milled in a hammer mill (LM 3100, Perten Instruments, Sweden) to obtain a standard whole grain quinoa flour that was used as reference flour.

2.2 Proximate composition

The average moisture content of the samples was measured by Official Method AACC 44-19 (AACC, 1999). Ash content was determined by incineration method, lipids content was carried out by gravimetric method using a Soxhlet apparatus with hexane as extraction solvent, and total protein content (N x 5.7) was analyzed by titrimetric method using a Kjeldahl distillation unit. Starch content was measured with the optional rapid method for total starch described by Englist et al. (Englyst, Hudson & Englyst, 2006).

2.3 Damaged starch and amylose content

The damaged starch content in quinoa samples was determined following the American Association of Cereal Chemists method (AACC, 2014) by using a Megazyme starch damage Kit (K-SDAM, Megazyme, Ireland) and it is referred at dry matter. Three replicates were made for each sample. Amylose content of the whole grain quinoa flour was determined by the lectin concanavalin A (Con A) method (Gibson, Solah, & McCleary, 1997) using the assay kit K-AMYL of Megazyme, Ireland. In both methods the absorbance was read at 510 nm.

2.4 Granulometry, color characteristics and bulk density

To determine the particle size distribution of the samples, a Mastersizer 3000 equipped with a dry dispersion unit (Malvern Instruments, Malvern, UK) was used. The particle size distribution was characterized by the median diameter (D_{50}) and the dispersion ($D_{90}-D_{10}$)/D_{50}) as described in Workineh et al. (Abebe, Collar, & Ronda, 2015).

Color measurements of quinoa samples were carried out using a colorimeter PCE-CSM5 (PCE Instruments, UK) on the basis of L^*, a^* and b^* values (L^* for the lightness from black (0) to white (100), a^* from green (−) to red (+), and b^* from blue (−) to yellow (+)) with 10º standard observer and D65 standard illuminant. The hue (h) and the chroma (C^*) were also obtained from the CIELAB coordinates. Each sample was measured five times.

Bulk density was determined according to Kaushal et al. (Kaushal, Kumar, & Sharma, 2012). Quinoa samples were carefully filled into previously tared 10 mL graduated cylinders. The cylinders were gently tapped up to constant level. Bulk density was calculated as mass of sample per unit volume of sample (kg/m^3). Each sample was measured in triplicate.

2.5 Least gelation concentration (LGC)

Least gelation concentration of quinoa samples was determined according to the method of Joshi et al. (Joshi, Liu, & Sathe, 2015). Test tubes containing suspensions of 2, 4, 6, 8, 10, 12, 14, 16, 18 and 20 g/100 mL of sample in 5 mL distilled water were heated in boiling water. After 1 h, the tubes were cooled under running water for some minutes followed by cooling at 4ºC for 2 h. Least gelation concentration was determined as the minimum concentration at which the sample did not fall down or slip when the test tube was inverted.

2.6 Techno-functional properties

Water-holding capacity (WHC) and water absorption capacity (WAC) of the samples were determined at 10% (w/v) following the method described by Abebe et al. (Abebe et al., 2015). The foaming capacity (FC) and foaming stability (FS) of the samples were also determined as described by Abebe et al. (Abebe et al., 2015) at 2% of concentration. Water absorption index (WAI), water solubility index (WSI) and swelling power (SP) of the quinoa samples, at 10% (w/v), were measured and calculated as described by Kaushal et al. (Kaushal et al., 2012) at three different temperatures: 60, 75 and 95 ºC to relate their behavior with their possible uses. Emulsifying activity (EA) was also determined at 25 and 80 ºC by the method given by Kaushal et al. (Kaushal et al., 2012) with some modifications. 6 g of sample were mixed with 100 mL of water and 100 mL of corn oil. The mixture was homogenized for 60 s using a homogenizer at 10000 rpm. The emulsion was evenly divided into 50 mL centrifuge tubes. Half of the tubes were directly centrifuged at 1300 g for 5 min to obtain the emulsifying activity at room temperature (25 ºC). The rest of the tubes were heated at 80 ºC for 30 min and centrifuged at 1300 g for 5 min to obtain the emulsifying activity at 80 ºC. In both cases the emulsifying activity was calculated by dividing the volume of the emulsified layer by the volume of the emulsion before centrifugation * 100.

2.7 Differential scanning calorimetry (DSC)

Gelatinization and retrogradation transitions were assessed by DSC (DSC3, STAR^e System, Mettler Toledo, Switzerland). Quinoa samples, ~6 mg, were weighed into aluminum pans (40 µl) and distilled water was added to achieve the ratio 30:70 (w:w, flour:water). The sample pans were kept for 1 h at room temperature for moisture equilibration and then scanned from 0 to 115 ºC at 5 ºC/min using an empty sealed pan as a reference. Onset (To), endset (Te) and peak (Tp) temperature (ºC) and enthalpy change (ΔH, J/g dry flour) of endothermic transitions were recorded. After the first run, the pans were stored at 4ºC for 14 days to follow the starch retrogradation. Endothermic transition of retrograded starch was determined using the same procedure. Each sample was measured in duplicate.

2.8 Pasting properties

Pasting properties of the samples were determined using a Kinexus Pro+ rheometer (Malvern Instruments, UK) equipped with a starch cell. Each quinoa sample (3.5 g, dry matter basis, dm) was mixed with 25 mL of deionized water before being loaded into the canister. The shear rate

was 160 rpm and the Standard 2 (STD2) programmed method (23 min) was used following the AACC International Method 76-21.02. The pasting temperature (PT), peak viscosity (PV), trough viscosity (TV), breakdown viscosity (BV = PV-TV), final viscosity (FV) and setback viscosity (SV = FV-TV) were recorded. The determination was carried out in duplicate.

2.9 Rheological properties of gels

The rheological tests were performed with a Kinexus Pro+ rheometer (Malvern Instruments, UK). The gel samples were made following the same procedure described for pasting tests. The gels were left to rest for 15 min to allow sample relaxation. Strain sweeps were carried out from 0.01 to 500% strain at 1 Hz of frequency. Frequency sweeps were carried out from 10 to 0.1 Hz in the linear viscoelastic region (LVR); the stress value chosen for the frequency sweep tests of all gels was 3.0 Pa, which was in the LVR. The frequency sweep data were fitted to power law as described by Ronda et al. (Ronda, Pérez-Quirce, Angioloni, & Collar, 2013). The fitting coefficients, G_1' and G_1'', and $(\tan \delta)_1$, represent the elastic and viscous moduli and the loss tangent, respectively, at a frequency of 1Hz. *a*, *b* and *c*, are the exponents of the corresponding potential equations and quantify the dependence of the elastic, viscous and loss tangent on the oscillation frequency. Each test was carried out at least in duplicate.

2.10 Statistical analysis

Statistical analyses were conducted using the software Statgraphics Centurion XVII-X64 (Bitstream, Cambridge, MN, USA). The analysis of the variance (ANOVA) by Least Significant Difference (LSD) at p-value ≤ 0.05 was determined.

3. Results and discussion

3.1 Proximate composition

The proximate composition of quinoa fractions and whole quinoa flour is presented in **Table 1**. It can be seen that the size reduction of quinoa seeds and sieving have a significant influence on the composition of flour fractions.. Similar results were found in the composition of whole grain quinoa flours from different geographic origin (Li, Wang, & Zhu, 2016). Among fractions, the moisture content ranged from 9.7 to 10.9%, thus, no important differences were observed. However, the medium fraction presented a significantly higher lipid (10.96% dry matter basis, dm), protein (23.54% dm) and ash (3.46% dm) content with respect to the other fractions and the whole grain flour, as a result of its germ enrichment (Mufari et al., 2018; Opazo-Navarrete, Tagle Freire, Boom, Janssen, & Schutyser, 2018). This indicates that the composition of the flours was substantially influenced by the milling and sieving processes. Ahmed et al. (Ahmed, Thomas, & Arfat, 2019) reported that protein and lipids content significantly increased in the finest particles (74 – 105 µm). Shullivan et al. (Sullivan, Engebertson, & Anderson (1960)) explained that the change in the protein content of hard wheat fractions of different size is not universal and it depends upon the structure of the endosperm (hard/soft) and type of endosperm cells (peripheral, prismatic or central). It should also depend on the milling equipment used for grinding the sample as each mill has a very different procedure to reduce the particle size. Ahmed et al. (2019) grinded the sample with a coffee bean mill while we used a ball mill. The cell-wall material from broken perisperm may contribute significantly to the ash content. The ash content of the coarse fraction (500-1000 µm) was significantly lower than that obtained in the other quinoa fractions. This was also observed by Ahmed et al. (Ahmed et al., 2019). The fine and the coarse fractions presented

a similar protein (≈13% dm) and lipids (≈ 5% dm) content, lower than the medium fraction, and therefore also similar amount of carbohydrates (≈79% dm), significantly higher than those found in quinoa grains. These findings demonstrate that the combination of dry milling (with a ball mill) and sieving allows to obtain a grit fraction (~500 µm) markedly enriched in protein, ash and lipids, with respect to the original grain, with a concentration 50% (for protein and ash) and 80% (for lipids) higher than the whole flour. This indicates that, beyond kinetic and flow considerations, the medium fraction (~500 µm) should be the best choice to use as raw material in supercritical carbon dioxide extraction of quinoa oil (Benito-Román et al., 2018; Solaesa et al., 2019; Wejnerowska & Ciaciuch, 2018). The medium fraction also represents a very suitable ingredient for both gluten free and vegetarian products due to its high protein and mineral content. The other two fractions, the ones of the smallest and largest particle sizes, with higher starch content and still with medium/high protein and lipids contents, could be used as ingredient in starch based food development with a specific particle size. Considering that quinoa grains are usually used boiled, the large size fraction could also be used directly in porridge or soups, or to other food applications.

Table 1. Chemical composition of quinoa samples

Sample	Yield (%)	Moisture (%)	Proteins (% dm)	Lipids (% dm)	Ash (% dm)	Starch (% dm)	Damaged starch (% dm)
Whole grain flour	-	9.91 ± 0.12 a	15.58 ± 0.94 b	6.14 ± 0.62 b	2.35 ± 0.25 b	63.2 ± 1.0 bc	6.5 ± 0.1 d
Fine fraction	11	10.86 ± 0.10 c	13.33 ± 0.65 a	5.16 ± 0.51 a	2.54 ± 0.47 b	63.1 ± 0.8 b	5.8 ± 0.1 c
Medium fraction	21	9.74 ± 0.11 a	23.54 ± 1.50 c	10.96 ± 0.80 c	3.46 ± 0.63 c	46.5 ± 1.4 a	2.2 ± 0.1 b
Coarse fraction	68	10.35 ± 0.09 b	13.27 ± 0.85 a	4.83 ± 0.64 a	2.09 ± 0.16 a	67.5 ± 2.1 c	1.9 ± 0.1 a

Data are the mean ± standard deviation (n = 2). Values with a letter in common in the same column are not significantly different ($p<0.05$); dm: dry matter basis

3.2 Damaged starch and amylose content

Table 1 presents the starch damage content determined in the quinoa samples. It can be seen that the smaller the particle size, the higher the content of damaged starch in the sample. The values ranged from 1.9 %, in the largest fraction to 5.8% in the finest fraction. These results were expectable since physical damage to starch is usually attributed to the dry-milling process (Lijuan, Guiying, Guoan, & Zaigui, 2007). The whole quinoa flour showed a starch damage of 6.5%, which is coherent with the smaller particle size obtained by hammer milling (see **Table 2**). This value was lower than other found in the literature for quinoa flour (~10 %) obtained with a different grinding mill (Srichuwong et al., 2017). The hammer mill seems to be less aggressive in damaging starch.

The amount of amylose estimated by Con A binding based method of whole quinoa flour was 10% ± 1 of the starch. This small value, also found in the three quinoa fractions, was in agreement with most studies, which reported values below 10% when the Con A method was used (Li & Zhu, 2017, 2018).

3.3 Granulometry, color characteristics and bulk density

Table 2 shows the median diameter (D_{50}) of particles of quinoa samples as well as their size dispersion ((D_{90} - D_{10})/D_{50}). The D_{50} varied in the following order: whole grain flour (116 µm) < fine fraction (171 µm) < medium fraction (493 µm) < coarse fraction (1220 µm). As could be

expected, the size dispersion of whole grain flour (2.92) was notably higher than those of the sieved fractions. The whole grain quinoa flour displayed a bimodal particle size distribution, with the first mode from 2 to 40 μm and the second one from 40 to 900 μm. A similar bimodal particle size distribution was observed in the fine fraction, while the medium and the coarse fractions presented a unimodal distribution. The narrowest size distribution was obtained in the middle fraction, with a size dispersion of 0.96, half than that of the fine fraction and 30% lower than that of the coarse one. It has been reported that the particle size distribution of flours depends on the grain's type and hardness, mill type and grinding time, which may explain the different reported distributions (Abebe et al., 2015; Ahmed, Al-Attar, & Arfat, 2016).

The color coordinates (L*, a*, b*, C* and h) of quinoa samples are also shown in **Table 2**. The lightness (L*) of the quinoa fractions increased with decreasing particle size, from 74.9 to 86.1%. The whole quinoa flour, with the smallest D_{50} value, had the highest luminosity, which could be associated with the increase of the surface area that would allow more light reflection (Ahmed et al., 2016). The hue angle (h) of the quinoa samples also varied from reddish to yellowish in the order: coarse fraction < medium = fine fractions < whole grain flour. The Chroma (C*) of the coarse (14.5) and medium (15.8) fractions were significantly higher than that of the fine fraction and the whole grain quinoa flour (≈12.1) indicating they had more vivid colors. Moreover, all the b* values were significantly lower than those reported by Ahmed et al. (Ahmed et al., 2019) for their quinoa samples, while our a* values were higher. This means that the quinoa flour studied by these authors was less reddish than ours, probably due to differences in the variety and cultivation conditions of quinoa used in both works.

The bulk density (kg/m^3) of the samples is included in **Table 2.** Bulk density of flours is important when considering its packaging and transport (Ratnawati, Desnilasari, Surahman, & Kumalasari, 2019). The results varied over a wide range of values, from 640 kg/m^3 for medium fraction to 781 kg/m^3 for the fine fraction. This could be related not only to the particle size of the samples, but also to their different composition (Abebe et al., 2015; Kaushal et al., 2012). In general, finer particles are able to compact better leaving less free space, so it was expected that the whole grain flour and the fine fraction had the highest bulk densities (749 kg/m^3 and 781 kg/m^3, respectively). However, the bulk density of the medium fraction was 640 kg/m^3, being the lowest. This value was probably related to the highest lipids and the lowest carbohydrate contents of this fraction. Other authors have also reported that bulk density has a positive correlation with carbohydrates content and a negative correlation with lipids (Kaushal et al., 2012; Ratnawati et al., 2019). The lowest moisture content (9.74%) of the medium fraction could also contribute to its low bulk density as moisture helps flour particles to stick together, thus reducing their specific volume (Kaushal et al., 2012; Ratnawati et al., 2019).

3.4 Least gelation concentration (LGC)

Least gelation concentration (LGC) of the samples ranged from 12 to 14 g/100 mL (**Table 2**). The lower the LGC, the better is the gelation ability of the sample (Kaushal et al., 2012). As it can be observed in **Table 2**, the whole grain flour and the medium fraction needed a higher concentration (14 g/100 mL) than the fine and the coarse fractions (12 g/100 mL) to form a relatively firm gel. The value of LGC depends on the type and content of proteins, carbohydrates and lipids, and the interactions among them (Kausal et al., 2012). The gelling capacity of flours, with a high starch and protein content, is influenced by the physical competition for water between proteins gelation and starch gelatinization (Kaushal et al., 2012). The presence of a high amount of lipids, as happened in the medium size fraction, should also have a high impact on the swelling

power of starch and its lower gelling ability. Starch, once gelatinized, also forms a gel in the retrogradation process. Therefore, in general, lower LGC values in flours mean a good gelation ability of the protein, a good swelling and gelation capacity of the starch or both.

Table 2. Physical and functional properties of quinoa samples

	Whole grain flour	**Fine fraction**	**Medium fraction**	**Coarse fraction**
Granulometry				
D_{50} (µm)	116 ± 2 a	171 ± 3 b	493 ± 3 c	1220 ± 6 d
$(D_{90} - D_{10})/D_{50}$	2.92 ± 0.1 d	1.81 ± 0.1 c	0.96 ± 0.1 a	1.38 ± 0.1 b
Color characterisitics				
L*	86.1 ± 0.3 d	81.2 ± 1.1 c	75.9 ± 0.6 b	74.9 ± 0.5 a
a*	2.7 ± 0.2 a	3.2 ± 0.3 b	4.3 ± 0.2 c	4.3 ± 0.3 c
b*	11.8 ± 0.4 a	11.7 ± 0.6 a	15.2 ± 0.5 c	13.8 ± 0.3 b
C*	12.0 ± 0.4 a	12.2 ± 0.6 a	15.8 ± 0.5 c	14.5 ± 0.2 b
h	76.8 ± 0.8 c	74.5 ± 0.7 b	74.5 ± 0.6 b	72.4 ± 0.9 a
Bulk density				
Bulk density (kg/m^3)	749 ± 18 c	781 ± 1 d	640 ± 5 a	702 ± 1 b
Functional properties				
LGC (g/100 mL)	14	12	14	12
WHC (g/g)	2.29 ± 0.29 a	2.31 ± 0.01 a	2.56 ± 0.17 a	2.39 ± 0.22 a
WAC (g/g)	0.94 ± 0.01 a	0.97 ± 0.02 a	1.60 ± 0.03 b	1.73 ± 0.09 c
FC (mL)	5 ± 2 a	7 ± 2 a	5 ± 2 a	4 ± 1 a
FS (%)	52 ± 5 b	56 ± 5 b	0 ± 0 a	51 ± 5 b
$EA_{25°C}$ (%)	62.5 ± 0 c	60.5 ± 3 c	50.0 ± 0 b	25.0 ± 0 a
$EA_{80°C}$ (%)	62.5 ± 0 c	62.5 ± 0 c	55.0 ± 4 b	30.0 ± 3 a
$SP_{95°C}$ (g/g)	7.12 ± 0.26 b	7.12 ± 0.15 b	6.34 ± 0.15 a	6.39 ± 0.10 a

D_{50}: median diameter; $(D_{90} - D_{10})/D_{50}$: size dispersion; *L**, *a**, *b**: CIELAB color coordinates; *C**: Chroma; h: hue; LGC: least gelation concentration; WHC: water holding capacity; WAC: water absorption capacity; FC: foaming capacity; FS: foaming stability; EA: emulsifying activity; SP: swelling power.

Data are the mean ± standard deviation (n = 3). Values with a letter in common in the same line are not significantly different ($p<0.05$)

3.5 Techno-functional properties

Results of WHC, WAC, foaming properties and emulsifying activity of the samples are also summarized in **Table 2**. Furthermore, WAI, WSI and SP were measured at 60, 75 and 95ºC to evaluate the behavior of the samples at different temperatures, and are shown in **Figure 1**. In general, the whole grain flour and the fine fraction presented very similar values in all the measured parameters. No significant differences were observed between the four samples in WHC values (~2.4 g of water /g of sample). When no force is applied, the samples had a similar behavior and the analysis method was not accurate enough to distinguish between them. However, WAC ranged from 0.94 to 1.73 g/g, increasing with particle size. In general, the water absorption capacity of flours increases with the reduction of particle size given that an increasing surface area enhances the interaction with water. However, our results showed the opposite trend with regard to particle size, probably because, in our case, the largest size fractions had the highest

protein (medium fraction) or starch (coarse fraction) contents, which markedly affect the WAC value (Ahmed et al., 2016; Ahmed et al., 2019). These results confirm that WAC can be influenced by many factors but, in particular, is significantly affected by the flour's composition (Ratnawati et al., 2019).

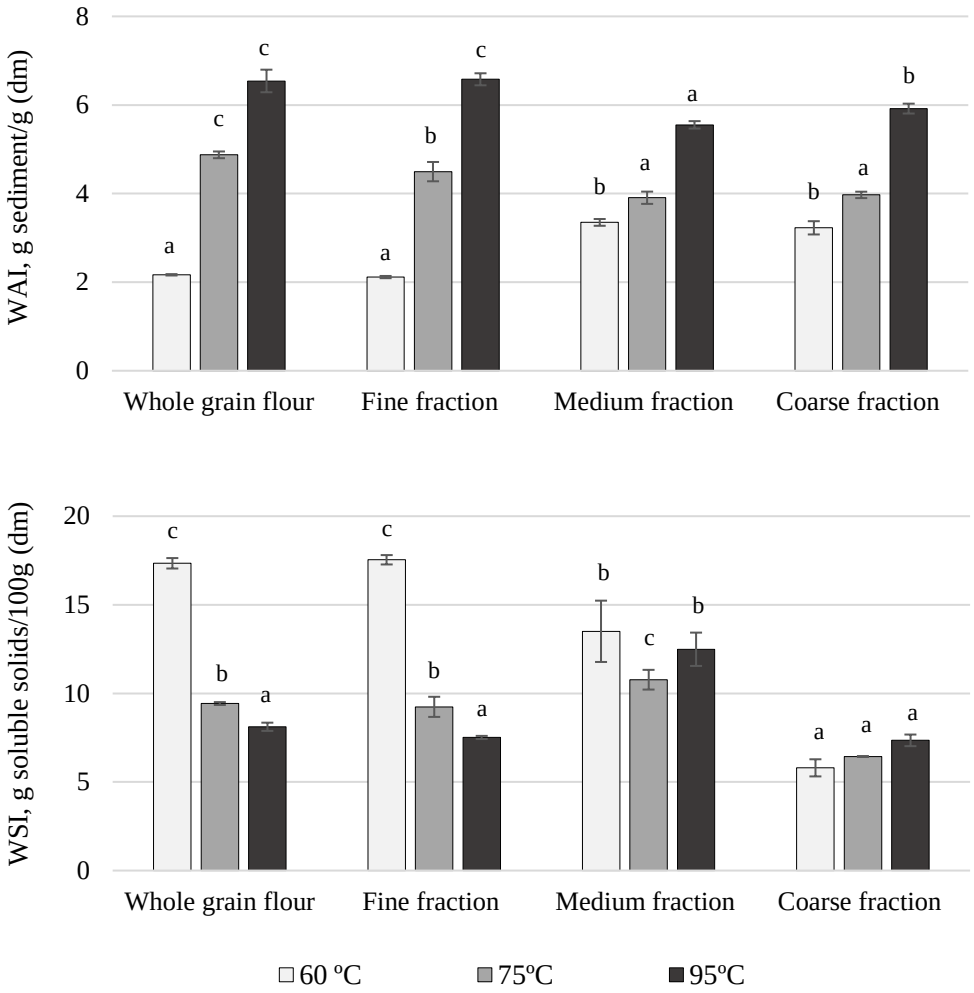

Figure 1. Water absorption index (WAI) and water solubility index (WSI) of quinoa samples, in function of temperature. The error bars represent the standard deviation. Bars with a letter in common for a same temperature represent not significantly different values among samples ($p<0.05$); dm: dry matter basis.

The foaming capacity of flours is mainly related to proteins, which form a continuous cohesive film around the air bubbles in the foam (Abebe et al., 2015; Kaushal et al., 2012), although foaming properties (capacity and stability) also show a negative relationship with lipid content (Shevkani, Singh, Kaur & Rana, 2014). No significant differences were observed between the four samples in the foaming capacity (~5 mL of foam). However, the foam formed by the medium fraction sample disappeared after 60 min of resting time while the other samples showed a FS above 50%. A high stability of the foam suggests that the native proteins soluble in the continuous phase (water) are very surface active in the flours. The very low foaming stability of the medium fraction could be explained by its high lipid content. The foaming capacity of the whole grain quinoa flour was below the values reported for other flours such as tef or wheat flours; however,

the foaming stability obtained for quinoa flour was above the values found in the literature for these other cereals (Abebe et al., 2015; Kaushal et al., 2012).

Emulsifying activity (EA) of the samples was measured at 25ºC and 80ºC to study the hypothetical behavior in raw and cooked applications and to quantify the stability of emulsions versus heat and time. Proteins can stabilize emulsions by electrostatic and steric repulsion on oil droplet surface (Kaushal et al., 2012). **Table 2** shows that EA values, ranging between 25% and 62.5%, were very similar at 25ºC and 80ºC denoting the high stability of these emulsions versus heat and time. The higher values of EA for the whole grain quinoa flour and the fine fraction and the lowest one for the coarse fraction suggest that the emulsifying ability of quinoa samples is also related to their particle size, which affects the accessibility of proteins to the oil-water interface.

In the four samples WAI increased with increasing temperature, ranging in the case of whole grain flour, from 2.17 to 6.54 g/g **(Figure 1)**. In general, WAI increased with the decrease of particle size at 75 and 95 °C. This increase could be explained by the concomitant increase of the surface area in the smaller particles that allows a higher interaction and absorption of water. However, some exceptions to this general trend were observed in the medium size fraction, which showed a slightly lower WAI value than that found in the coarse fraction. It can be explained by the different composition of the fraction, mainly protein, fiber and starch that also influences hydration properties. The damaged starch could be another reason for the increase of WAI in flours. A similar observation relating WAI with particle size and composition was reported by Ahmed et al. (Ahmed et al., 2019).

The WSI was significantly ($p<0.05$) dependent on the quinoa fraction and the temperature of the measurement (**Figure 1**). The double effect (sample x temperature) was also significant on the results obtained ($p<0.05$) (data not shown): the effect of the temperature was different depending on the studied fraction. The solubilized material of quinoa flour may include various components such as starch, protein, dietary fiber, minerals and phenolics (Li & Zhu, 2017). A great diversity in the swelling and solubility patterns among quinoa samples has been observed. Apart from starch, the dissolved protein may also contribute to the WSI. For some samples, such as whole grain flour and fine fraction, WSI decreased with increasing temperature from ~17.5% at 60ºC to ~8% at 95ºC. A possible explanation could be the denaturation of dissolved proteins, such as albumins (~64ºC), and globulins (~94ºC) (Li & Zhu, 2017). At 60ºC both proteins were solubilized, so WSI showed the highest value. At 75ºC, albumins were denatured but not globulins resulting in an intermedium value of WSI. However, at 95ºC both proteins were denatured; therefore, the WSI value was the lowest. For coarse fraction, WSI increased with increasing temperature. The low WSI values found in this fraction and their increase with temperature suggest that they might be more influenced by the large particle size than by the fraction's composition. Similar results were shown by Ahmed et al. (Ahmed et al., 2019) for a quinoa fraction with large particle size. Besides, the coarse fraction had a higher starch content, so at 75ºC and 95ºC a greater quantity of soluble starch was produced than at 60ºC. For the medium fraction, WSI firstly decreased with temperature, from 60 to 75ºC, but later increased at 95ºC. The two factors of influence studied, i.e., composition and particle size, probably have an effect on WSI which importance depend on the temperature. The particular composition of this fraction and its intermedium size can justify its particular swelling and solubility pattern. **Table 2** summarizes the SP values obtained at 95ºC. As expected, in all samples SP followed the same tendency versus temperature and presented similar values to WAI (data not shown).

3.6 Thermal properties

Gelatinization data obtained from DSC are shown in **Table 3.** Thermograms of quinoa samples showed two wide endothermic transitions in the first run; one between 65 and 80°C, due to starch gelatinization, and the other between 85 and 100°C, related to amylose-lipid complex and/or protein denaturation (Solaesa et al., 2019). The reversibility of this second endotherm (Tp~95ºC) confirms the presence of amorphous amylose-lipid complex within these samples (Eliasson, 1994). Variations in gelatinization enthalpy of the different quinoa samples were related to their different particle size and starch content: the medium fraction, with the lowest amount of starch, had the lowest gelatinization enthalpy (6.1 ± 0.2 J/g dm) while the coarse fraction had the highest (9 ± 0.3 J/g dm), although no direct proportionality between the two properties was observed. No significant differences among gelatinization temperatures (To~62ºC, Tp~70ºC, Te~80ºC) of quinoa samples, regardless of their different particle size and composition, were observed. This means that there is a uniform starch structure within the quinoa grain or at least, the differences are not large enough to significantly affect the gelatinization phenomenon (Ahmed et al., 2019). However, the width of the gelatinization peak, Te – To, increased with the size of quinoa samples, indicating that the gelatinization process requires a higher temperature range to be accomplished in larger particles. The dissociation enthalpies of amylose-lipid inclusion complexes obtained in the first run were similar for all quinoa samples, ~ 0.7 J/g dm, except for the coarse fraction where it was significantly lower (0.3 J/g dm). However, in the second run the enthalpy of this transition increased, in the whole flour and the fine fraction, up to 1.5 J/g dm, while presented the same value in the coarse and medium fractions (see **Figure 2**). Eliasson (Eliasson, 1994) reported that the increased values during the second scan are due to better conditions for complex formation after the first heating. It is related to the leaking of amylose out of the granules that occurs at temperatures above gelatinization temperature range. Our results demonstrate that amylose-lipid complex formation is also affected by the flour's particle size. Lipids within the medium and coarse fractions were less available to interact with amylose than in the fine fraction and the whole quinoa flour. An opposite effect of the flour's particle size was observed on the melting enthalpy of retrograded amylopectin, the other endotherm obtained in the second scan, performed after 14 days of sample storage at 4ºC. While the temperature of this transition did not differ significantly between samples, meaning that it did not depend on the composition of the fraction, its enthalpy increased with the size of the particles. It followed the order: whole grain flour (0.39 J/g dm) ≈ fine fraction (0.36 J/g dm) < medium fraction (0.99 J/g dm) <coarse fraction (2.4 J/g dm). Under certain conditions, amylopectin may also participate in the formation of lipid inclusion complexes (Eliasson, 1994) which would prevent its recrystallization. This would explain the low retrogradation, even after 14 days of storage, of amylopectin in quinoa flour, a property already described by other authors (Putseys, Lamberts, & Delcour, 2010). However, in samples with large particle size, the lipids could not interact with either amylose or amylopectin, which led to a higher degree of amylopectin retrogradation at the same time as a lower formation of the amylose-lipid complex. To clarify this issue, the coarse fraction was milled with a coffee grinder to reduce its particle size prior to performing the same two scans again in order to compare two samples with the exact same chemical composition. **Figure 2** includes, as isolated points, the new values obtained for the same coarse fraction after reducing its size to 315μm (D_{50}). The new enthalpies obtained for the two studied transitions were significantly different than the previous ones and near to the values obtained for the medium fraction (D_{50} = 493μm). These results allowed us to confirm the significant effect of particle size on the enthalpy of these thermal transitions.

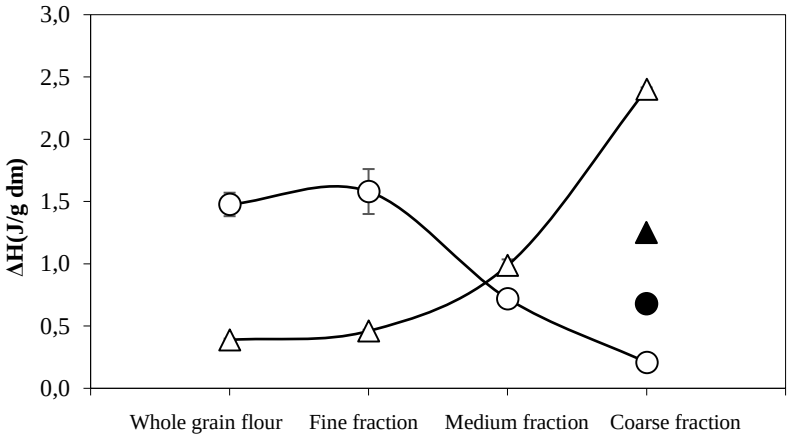

Figure 2. Effect of the particle size of the samples on the starch retrogradation (triangles) and amylose-lipid melting (circles) enthalpies. Coarse fraction milled were represented by solid black symbols. The error bars represent the standard deviation

Table 3. Gelatinization, pasting and rheological properties of gels of quinoa samples (all viscoelastic parameters were measured at 25ºC).

	Whole grain flour	**Fine fraction**	**Medium fraction**	**Coarse fraction**
Thermal properties				
ΔH (J/g dm)	6.72 ± 0.16 b	7.45 ± 0.14 c	6.10 ± 0.16 a	9.04 ± 0.33 d
To (ºC)	62.34 ± 1.02 a	63.22 ± 0.20 a	62.45 ± 0.36 a	61.48 ± 1.27 a
Tp (ºC)	70.45 ± 0.86 a	70.88 ± 0.27 a	70.86 ± 0.19 a	70.31 ± 1.09 a
Te (ºC)	79.10 ± 1.18 a	80.17 ± 1.01 a	80.05 ± 0.06 a	80.05 ± 1.81 a
Te - To (ºC)	16.75 ± 0.21 a	16.95 ± 0.78 a	17.6 ± 0.42 ab	19 ± 1.08 b
Pasting properties				
PT (ºC)	76.1 ± 0.2 a	77.1 ± 0.1 a	79.8 ± 0.2 b	87.0 ± 1.4 c
PV (Pa·s)	2.69 ± 0.07 c	2.34 ± 0.01 b	1.01 ± 0.01 a	-
TV (Pa·s)	2.02 ± 0.03 c	1.71 ± 0.03 b	0.99 ± 0.01 a	-
BV (Pa·s)	0.67 ± 0.04 b	0.63 ± 0.02 b	0.03 ± 0.04 a	-
SV (Pa·s)	0.77 ± 0.01 b	1.02 ± 0.03 c	0.37 ± 0.01 a	-
FV (Pa·s)	2.78 ± 0.02 b	2.73 ± 0.04 b	1.36 ± 0.01 a	3.52 ± 0.09 c
Rheological properties				
G' (Pa)	322 ± 18 a	412 ± 14 a	293 ± 33 a	3826 ± 381 b
a	0.060 ± 0.002 a	0.053 ± 0.002 a	0.087 ± 0.008 b	0.077 ± 0.001 b
G'' (Pa)	33 ± 1 a	40 ± 1 a	45 ± 6 a	729 ± 20 b
b	0.335 ± 0.001 d	0.302 ± 0.009 c	0.269 ± 0.002 b	0.140 ± 0.001 a
tan δ_1	0.103 ± 0.003 a	0.098 ± 0.001 a	0.155 ± 0.004 b	0.191 ± 0.014 c
c	0.275 ± 0.001 d	0.249 ± 0.007 c	0.182 ± 0.009 b	0.063 ± 0.002 a
Cross over (Pa)	52 ± 4 ab	67 ± 2 b	36 ± 3 a	126 ± 17 c
τ max (Pa)	12 ± 1 ab	15 ± 1 b	5 ± 2 a	14 ± 3 ab

ΔH: Gelatinization enthalpy; To: onset temperature; Tp: peak temperature; Te: endset temperature; PT: Pasting temperature; PV: Peak viscosity; Trough viscosity; BV: Breakdown viscosity; SV: Setback viscosity; FV: Final viscosity. G', G'' and $(\tan \delta)_1$: elastic and viscous moduli and the loss tangent at a frequency of 1 Hz. The a, b and c exponents: quantify the dependence degree of dynamic moduli and the loss tangent with the oscillation frequency. τ_{max}

: maximum stress that samples can tolerate in the LVR. Data are the mean ± standard deviation (n = 2). Values with a letter in common in the same line are not significantly different ($p<0.05$); dm: dry matter basis.

3.7 Pasting properties

The pasting profile of a flour is an effective method for relating starch functionality with its structural characteristics and the potential industrial application in products, since it depends on its viscosity and thickening behavior. **Figure 3** and **Table 3** demonstrated that each quinoa sample has unique pasting and viscosity properties. It is well known that several pasting parameters of flour are positively correlated with apparent amylose content (Li & Zhu, 2017). Therefore, it should be taken into account that the content of amylose in the quinoa starch is low (10%), so the pasting profile of quinoa samples is not expected to present a high viscosity, compared to other starch-rich cereals. The peak viscosity (2.69 Pa·s), trough viscosity (2.02 Pa·s) and breakdown viscosity (0.67 Pa·s) were higher in the whole grain flour than in the rest of samples. These values were similar to other quinoa flours found in literature (Li & Zhu, 2017). The pasting temperature (PT), or temperature required by starch granules to start swelling, decreased systematically from 87 to 76°C with decreasing particle size, indicating that smaller particles hydrate easier than the larger ones. As it can be seen in **Figure 3,** the coarse fraction, in spite of its highest starch content, did not show a peak nor a valley in the pasting curve, but a continuous increasing curve along the whole test that led to the highest FV (3.52 Pa·s). This indicates that water takes longer than the duration of the test to pass through the large structures and reach the starch granules to allow them to swell and to produce a rapid increase in viscosity (PV). The medium fraction showed the lowest PV (1.01 Pa·s) and a BV near zero. It could be due to the low amount of starch in this fraction and its high lipids and proteins content, which difficult the access of water to the starch granules hindering its swelling and increasing its stability versus heating and stirring (Opazo-Navarrete et al., 2018).

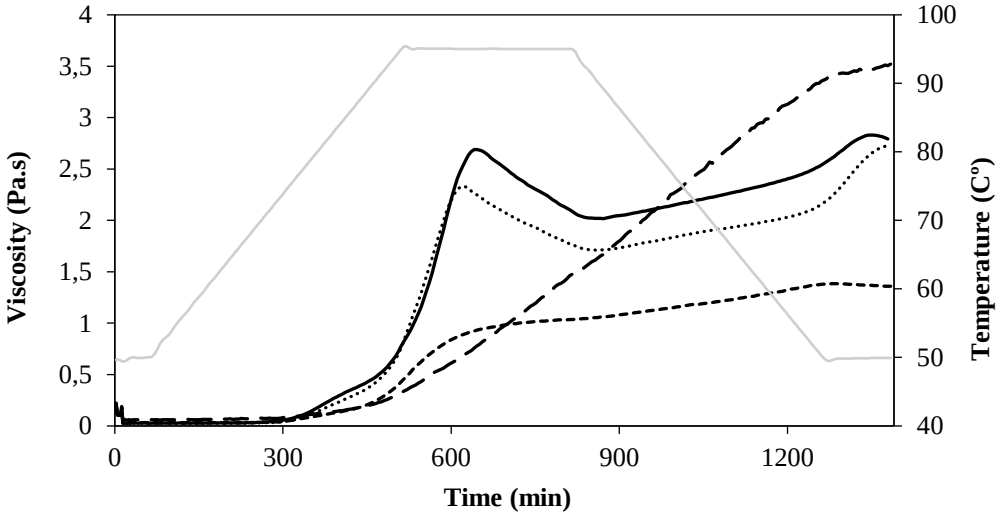

Figure 3. Pasting profiles of quinoa samples. Whole grain quinoa flour (——), Fine fraction ~200 µm (….), Medium fraction ~500 µm (----), Coarse fraction ~1000 µm (— —). The grey line corresponds to temperature (ºC).

3.8 Rheological properties of the gels

The rheological properties of the gels formed from quinoa samples are also summarized in **Table 3.** It presents the fitting parameters of the frequency sweeps versus frequency carried out in the

linear viscoelastic region (LVR) to power law. The strain sweeps assays carried out to establish the LVR showed two different regions in quinoa gels, LVR in which G' and tan δ values were nearly constant, and the non-linear domain in which G' started to decrease, and at the same time the tan δ began to increase with strain until the curves of G' and G" intersected (G'=G'' and tan δ = 1) (see **Figure 4**). The maximum stress, τ_{max}, gels resist before their structure disruption, at the end of LVR, is also showed in **Table 3**. The gel formed with the medium fraction presented the lowest τ_{max} (5 Pa), indicating a weaker structure which breaks easier under stress. It may be attributed to its low amount of starch concomitant to its high protein and lipids content. The stress at which the gels passed from solid like to viscous like behavior (the crossing point of the curves) is also informed in this table. Villanueva et al. (Villanueva, De Lamo, Harasym, & Ronda, 2018) also observed in gels made from pure starch-protein blends, that the presence of proteins reduced the resistance of the gels to breakage and led to lower τ_{max} values than those of protein-free gels (Villanueva, De Lamo, et al., 2018). As can be seen in **Figure 4** and **Table 3** the coarse fraction led to the most consistent gels, with the highest elastic (G') and viscous (G") moduli. Their values at 1 Hz (G_1' and G_1") were around ten and twenty times higher than those obtained for the gels made from the other quinoa fractions. This is probably due to the synergistic effect of a significantly higher amount of starch and the big particle size of the fraction (Ahmed et al., 2019). The coarse fraction led to gels with a slightly higher tan δ value, which means it had a lower solid like behavior than the other quinoa samples. Nevertheless, the low tan δ_1 values (0.10-0.19) of all samples allow to classify them as "true" gels (Villanueva, Ronda, Moschakis, Lazaridou, & Biliaderis, 2018). Frequency sweeps from 0.1 to 10 Hz showed that in all the gel samples, G' and G'' increased with frequency, although faster for the viscous modulus (b=0.14–0.34) than for the elastic one (a=0.05–0.09). Despite the evident differences in composition and particle size among the fine and medium fractions and the whole quinoa sample, non-significant differences were observed in their rheological behavior. It can be concluded that the medium fraction, enriched in proteins and lipids, is suitable for use in the preparation of enriched pasta. The high consistency of gels made from the quinoa coarse fraction broadens the applicability of this pseudocereal as thickener in desserts, sauces or in gels-based food products.

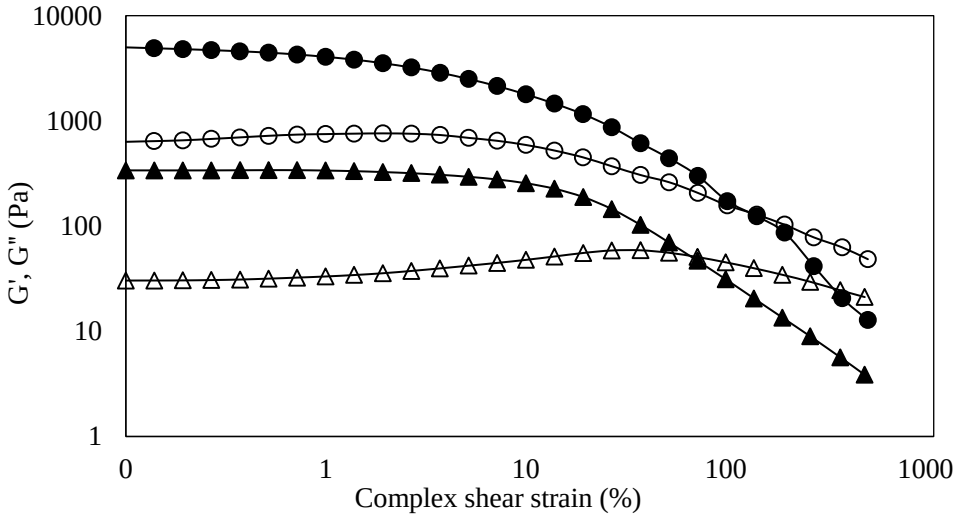

Figure 4. Strain sweeps of whole grain quinoa flour (triangles) and course fraction (circles) gels. The elastic modulus, G', is represented using solid symbols and the viscous modulus, G'', with open symbols.

4. Conclusion

Separated particle fractions of quinoa flour showed wide variations in the proximate composition and functionality. The fine fraction showed the most similar functional, pasting and rheological properties to the whole grain quinoa flour. The medium size fraction, with the desired particle size for pasta making and an efficient supercritical oil extraction (~500 µm) resulted to be richer in protein, lipids and ash while the coarse fraction was enriched in carbohydrates. Techno-functional, pasting and thermal properties of the quinoa fractions were strongly influenced by their different particle size and composition. However, the rheological properties of gels made from the fine and medium fractions were very similar to each other despite their different composition, and in turn, very similar to those of gels made from whole quinoa. On the contrary, the coarse fraction led to much more consistent gels with elastic and viscous moduli ten and twenty times higher than the standard, whole grain quinoa flour. Therefore, it can be concluded that dry fractionation of quinoa grains is a feasible procedure to tailoring the nutritional profile of the flour and its techno-functional and rheological properties.

Acknowledgements

The authors are grateful for the financial support of the Ministerio de Economía y Competitividad and the European Regional Development Fund (FEDER) (AGL2015-63849-C2-2-R) and the Junta de Castilla y León/FEDER (VA072P17). We thank Sagrario Beltran and Teresa Sanz (UIC 128) by their technical support. We also thank IESMAT (Madrid, España) for the determination of the particle size distribution of quinoa samples with Mastersizer 3000. Antonio J. Vela thanks to the Junta de Castilla y León for his pre-doctoral grant.

References

AACC. (1999). AACC International Methods, 44-19.01. Moisture-Air-Oven Method. *AACC International Approved Methods*. https://doi.org/10.1016/j.beem.2005.04.006

AACC. (2000). AACC International Methods, 76-21.01. Anonymous approved methods of the AACC (10th ed.). St. Paul: The Association.

AACC. (2014). AACC International Method, 76-31.01. Determination of Damaged Starch-Spectrophotometric Method. *AACC International Approved Methods*. https://doi.org/10.1094/AACCIntMethod-76-33.01

Abebe, W., Collar, C., & Ronda, F. (2015). Impact of variety type and particle size distribution on starch enzymatic hydrolysis and functional properties of tef flours. *Carbohydrate Polymers*, *115*, 260–268. https://doi.org/10.1016/j.carbpol.2014.08.080

Abugoch James, L. E. (2009). Quinoa (Chenopodium quinoa Willd.): Composition, chemistry, nutritional, and functional properties. In *Advances in Food and Nutrition Research* (Vol. 58, pp. 1–31). https://doi.org/10.1016/S1043-4526(09)58001-1

Ahmed, J., Al-Attar, H., & Arfat, Y. A. (2016). Effect of particle size on compositional, functional, pasting and rheological properties of commercial water chestnut flour. *Food Hydrocolloids*, *52*, 888–895. https://doi.org/10.1016/j.foodhyd.2015.08.028

Ahmed, J., Thomas, L., & Arfat, Y. A. (2019). Functional, rheological, microstructural and antioxidant properties of quinoa flour in dispersions as influenced by particle size. *Food Research International*, *116*(June 2018), 302–311.

https://doi.org/10.1016/j.foodres.2018.08.039

Ando, H., Chen, Y.-C., Tang, H., Shimizu, M., Watanabe, K., & Mitsunaga, T. (2002). Food Components in Fractions of Quinoa Seed. *Food Science and Technology Research*, *8*(1), 80–84. https://doi.org/10.3136/fstr.8.80

Bazile, D., & Baudron, F. (2013). The dynamics of the global expansion of quinoa growing in view of its high biodiversity. *State of the Art Report on Quinoa around the World* , (April), 42–56. Retrieved from www.fao.org/publications

Benito-Román, O., Rodríguez-Perrino, M., Sanz, M. T., Melgosa, R., & Beltrán, S. (2018). Supercritical carbon dioxide extraction of quinoa oil: Study of the influence of process parameters on the extraction yield and oil quality. *Journal of Supercritical Fluids*, *139*(May), 62–71. https://doi.org/10.1016/j.supflu.2018.05.009

Cocozza, C., Pulvento, C., Lavini, A., Riccardi, M., d'Andria, R., & Tognetti, R. (2013). Effects of increasing salinity stress and decreasing water availability on ecophysiological traits of quinoa (Chenopodium quinoa Willd.) grown in a mediterranean-type agroecosystem. *Journal of Agronomy and Crop Science*, *199*(4), 229–240. https://doi.org/10.1111/jac.12012

Contreras-Jiménez, B., Torres-Vargas, O. L., & Rodríguez-García, M. E. (2019). Physicochemical characterization of quinoa (Chenopodium quinoa) flour and isolated starch. *Food Chemistry*, *298*(May). https://doi.org/10.1016/j.foodchem.2019.124982

Eliasson, A. C. (1994). Interactions between starch and lipids studied by DSC. *Thermochimica Acta*, *246*(2), 343–356. https://doi.org/10.1016/0040-6031(94)80101-0

Englyst, K.N., Hudson, G.J., Englyst, H.N. (2006). Starch analysis in food. In: Meyers, R.A. (Ed.), *Encyclopedia of Analytical Chemistry*. John Wiley & Sons,Chichester, pp. 4246-4262

García-Salcedo, Á. J., Torres-Vargas, O. L., & Ariza-Calderón, H. (2017). Physical-chemical characterization of quinoa (Chenopodium quinoa Willd.), amaranth (Amaranthus caudatus L.), and chia (Salvia hispanica L.) flours and seeds. *Acta Agronomica*, *67*(2). https://doi.org/10.15446/acag.v67n2.63666

Gibson, T. S., Solah, V. A., & McCleary, B. V. (1997). A procedure to measure amylose in cereal starches and flours with concanavalin A. *Journal of Cereal Science*, *25*(2), 111–119. https://doi.org/10.1006/jcrs.1996.0086

Jacobsen, S. E. (2003). The worldwide potential for quinoa (Chenopodium quinoa Willd.). *Food Reviews International*, *19*(1–2), 167–177. https://doi.org/10.1081/FRI-120018883

Joshi, A. U., Liu, C., & Sathe, S. K. (2015). Functional properties of select seed flours. *LWT - Food Science and Technology*, *60*(1), 325–331. https://doi.org/10.1016/j.lwt.2014.08.038

Joubert, M., Morel, M. H., & Lullien-Pellerin, V. (2018). Pasta color and viscoelasticity: Revisiting the role of particle size, ash, and protein content. *Cereal Chemistry*, *95*(3), 386–398. https://doi.org/10.1002/cche.10038

Kaushal, P., Kumar, V., & Sharma, H. K. (2012). Comparative study of physicochemical, functional, antinutritional and pasting properties of taro (Colocasia esculenta), rice (Oryza sativa) flour, pigeonpea (Cajanus cajan) flour and their blends. *LWT - Food Science and Technology*, *48*(1), 59–68. https://doi.org/10.1016/j.lwt.2012.02.028

Li, G., Wang, S., & Zhu, F. (2016). Physicochemical properties of quinoa starch. *Carbohydrate Polymers*, *137*, 328–338. https://doi.org/10.1016/j.carbpol.2015.10.064

Li, G., & Zhu, F. (2017). Physicochemical properties of quinoa flour as affected by starch interactions. *Food Chemistry*, *221*, 1560–1568. https://doi.org/10.1016/j.foodchem.2016.10.137

Li, G., & Zhu, F. (2018). Quinoa starch: Structure, properties, and applications. *Carbohydrate*

Polymers, *181*(September 2017), 851–861. https://doi.org/10.1016/j.carbpol.2017.11.067

Lijuan, S., Guiying, Z., Guoan, Z., & Zaigui, L. (2007). Effects of different milling methods on flour quality and performance in steamed breadmaking. *Journal of Cereal Science*, *45*(1), 18–23. https://doi.org/10.1016/j.jcs.2006.02.004

Mastromatteo, M., Chillo, S., Civica, V., Iannetti, M., Suriano, N., & Del Nobile, M. A. (2012). A multistep optimization approach for the production of healthful pasta based on nonconventional flours. *Journal of Food Process Engineering*, *35*(4), 601–621. https://doi.org/10.1111/j.1745-4530.2010.00610.x

Mufari, J. R., Miranda-Villa, P. P., & Calandri, E. L. (2018). Quinoa germ and starch separation by wet milling, performance and characterization of the fractions. *Lwt*, *96*(June), 527–534. https://doi.org/10.1016/j.lwt.2018.06.010

Opazo-Navarrete, M., Tagle Freire, D., Boom, R. M., Janssen, A. E. M., & Schutyser, M. A. I. (2018). Dry fractionation of quinoa sweet varieties Atlas and Riobamba for sustainable production of protein and starch fractions. *Journal of Food Composition and Analysis*, *74*(September), 95–101. https://doi.org/10.1016/j.jfca.2018.09.009

Pellegrini, M., Lucas-Gonzales, R., Ricci, A., Fontecha, J., Fernández-López, J., Pérez-Álvarez, J. A., & Viuda-Martos, M. (2018). Chemical, fatty acid, polyphenolic profile, techno-functional and antioxidant properties of flours obtained from quinoa (Chenopodium quinoa Willd) seeds. *Industrial Crops and Products*, *111*(July 2017), 38–46. https://doi.org/10.1016/j.indcrop.2017.10.006

Pereira, E., Encina-Zelada, C., Barros, L., Gonzales-Barron, U., Cadavez, V., & C.F.R. Ferreira, I. (2019). Chemical and nutritional characterization of Chenopodium quinoa Willd (quinoa) grains: A good alternative to nutritious food. *Food Chemistry*, *280*(December 2018), 110–114. https://doi.org/10.1016/j.foodchem.2018.12.068

Prego, I., Maldonado, S., & Otegui, M. (1998). Seed structure and localization of reserves in Chenopodium quinoa. *Annals of Botany*, *82*(4), 481–488. https://doi.org/10.1006/anbo.1998.0704

Putseys, J. A., Lamberts, L., & Delcour, J. A. (2010). Amylose-inclusion complexes: Formation, identity and physico-chemical properties. *Journal of Cereal Science*, *51*(3), 238–247. https://doi.org/10.1016/j.jcs.2010.01.011

Ratnawati, L., Desnilasari, D., Surahman, D. N., & Kumalasari, R. (2019). Evaluation of Physicochemical, Functional and Pasting Properties of Soybean, Mung Bean and Red Kidney Bean Flour as Ingredient in Biscuit. *IOP Conference Series: Earth and Environmental Science*, *251*(1). https://doi.org/10.1088/1755-1315/251/1/012026

Ronda, F., Pérez-Quirce, S., Angioloni, A., & Collar, C. (2013). Impact of viscous dietary fibres on the viscoelastic behaviour of gluten-free formulated rice doughs: A fundamental and empirical rheological approach. *Food Hydrocolloids*, *32*(2), 252–262. https://doi.org/10.1016/j.foodhyd.2013.01.014

Shevkani, K., Singh, N., Kaur, A., Rana J.C. (2014). Physicochemical, Pasting, and Functional Properties of Amaranth Seed Flours: Effects of Lipids Removal. *Journal of Food Science*, *79*(7), 1271-1277. doi: 10.1111/1750-3841.12493.

Solaesa, Á. G., Villanueva, M., Beltrán, S., & Ronda, F. (2019). Characterization of Quinoa Defatted by Supercritical Carbon Dioxide. Starch Enzymatic Susceptibility and Structural, Pasting and Thermal Properties. *Food and Bioprocess Technology*, *12*(9), 1593–1602. https://doi.org/10.1007/s11947-019-02329-4

Sosa, M., Califano, A., & Lorenzo, G. (2019). Influence of quinoa and zein content on the

structural, rheological, and textural properties of gluten-free pasta. *European Food Research and Technology*, *245*(2), 343–353. https://doi.org/10.1007/s00217-018-3166-5

Srichuwong, S., Curti, D., Austin, S., King, R., Lamothe, L., & Gloria-Hernandez, H. (2017). Physicochemical properties and starch digestibility of whole grain sorghums, millet, quinoa and amaranth flours, as affected by starch and non-starch constituents. *Food Chemistry*, *233*, 1–10. https://doi.org/10.1016/j.foodchem.2017.04.019

Stikic, R., Glamoclija, D., Demin, M., Vucelic-Radovic, B., Jovanovic, Z., Milojkovic-Opsenica, D., Milovanovic, M. (2012). Agronomical and nutritional evaluation of quinoa seeds (Chenopodium quinoa Willd.) as an ingredient in bread formulations. *Journal of Cereal Science*, *55*(2), 132–138. https://doi.org/10.1016/j.jcs.2011.10.010

Sullivan, B., Engebretson, W.E., Anderson, M.L. (1960). The relation of Particle Size to Certain Flour Characteristics. *Cereal Chemistry*, *37*, 436-455.

Sun, Y., Liu, F., Bendevis, M., Shabala, S., & Jacobsen, S. E. (2014). Sensitivity of Two Quinoa (ChenopodiumquinoaWilld.) Varieties to Progressive Drought Stress. *Journal of Agronomy and Crop Science*, *200*(1), 12–23. https://doi.org/10.1111/jac.12042

Villanueva, M., De Lamo, B., Harasym, J., & Ronda, F. (2018). Microwave radiation and protein addition modulate hydration, pasting and gel rheological characteristics of rice and potato starches. *Carbohydrate Polymers*, *201*(June), 374–381. https://doi.org/10.1016/j.carbpol.2018.08.052

Villanueva, M., Ronda, F., Moschakis, T., Lazaridou, A., & Biliaderis, C. G. (2018). Impact of acidification and protein fortification on thermal properties of rice, potato and tapioca starches and rheological behaviour of their gels. *Food Hydrocolloids*, *79*, 20–29. https://doi.org/10.1016/j.foodhyd.2017.12.022

Wang, S., & Zhu, F. (2016). Formulation and Quality Attributes of Quinoa Food Products. *Food and Bioprocess Technology*, *9*(1), 49–68. https://doi.org/10.1007/s11947-015-1584-y

Wejnerowska, G., & Ciaciuch, A. (2018). Optimisation of oil extraction from Quinoa seeds with supercritical carbon dioxide with co-solvents. *Czech Journal of Food Sciences*, *36*(1), 81–87. https://doi.org/10.17221/122/2017-CJFS

Zhu, F., & Li, H. (2019). Modification of quinoa flour functionality using ultrasound. *Ultrasonics Sonochemistry*, *52*(October), 305–310. https://doi.org/10.1016/j.ultsonch.2018.11.027